1 LASER

LASER is a E^{2}TLA[1] for Light Amplification by Stimulated Emission. The LASER used in PHYS-339 is a solid-state LASER with an output claimed of less than 1 mW. The properties of the photons emitted by the LASER are listed in figure(1). The wide range is an indication of manufacturing variation, each individual LASER will have a sharply defined wavelength.

Wavelength	630–680 nm
Frequency	441–476 THz
Energy	1.82–1.97 eV

Figure 1: Properties of photon emitted by solid-state Laser

The solid-state laser is special case of a *Light Emitting Diode*, which is itself a special case of a *P-N junction.* A P-N junction is a region of P-doped semiconductor in electrical contact with a region of N-doped semiconductor.

1.1 Semiconductor Physics

I assume the reader is familiar with the energy levels in a single atom. One important aspect of solid-state physics is the crystal structure of solids. For example, silicon (^{14}Si) has a diamond crystal structure, with a lattice spacing of 0.543 nm[1]. Thus one can solve Schrödinger's equation for a periodic potential. One interesting result of this is that the quantized energy levels of each isolated atom are shifted and combine such that there are bands of allowed energies and bands of forbidden energies. Most of the bands correspond to electrons bound to individual atoms within the bulk, but there is a band which corresponds to electrons which are free to move within the bulk. These are called free electrons, and the energy band is called the conduction band. The next important concept is the *Fermi Energy*, is simple terms, this is the energy level of the highest energy electron in the lowest energy state of the solid, i.e. at absolute zero. If the fermi energy falls inside the conduction band, then the material will always have conduction electrons and we call it a metal. If the fermi energy falls below the conduction band then at low temperatures there will be no conduction electrons. The gap between the lowest energy in the conduction band and the highest energy in the band below, called the *Valence Band* is called the *band gap*. Materials which have a small enough band gap will, at room temperature, promote a small number of electrons to the conduction band via thermal excitation. These materials are called semiconductors. Semiconductors exhibit a negative coefficent of resistance, as temperature increases, the number of electrons in the conduction band increases and thus the resistance decreases. Another interesting feature of materials with a band gap is that for each electron promoted into the conduction band, a hole is left in the valence band. This hole, where an electron used to be, is also free to move

[1]Extended Extended Three Letter Acronym

within the bulk. If we have a piece of semiconductor in an electric field, and a electron-hole pair is created thermally (by the absorbtion of either a phonon or a photon), then the electron will drift in on direction and the hole will drift in the other. Both act as charge carriers. The hole usually moves slightly slower because it has a slightly larger effective mass.

It is possibly to calculate the number of charge carriers at a given temperature for a semiconductor with a given band gap. It is probably easiest to see graphically. Figure 2 shows the energy density of carriers in silicon at 300 K, figure 3 shows silicon at 500 K. The bottom curve is the fermi probability distribution,

$$f_F(E) = \frac{1}{1 + e^{\frac{E - E_F}{kT}}}. \qquad (1)$$

The middle set of curves show the density of states. This should have been covered by a statistical mechanics course, the important result being that in a 3-dimensional system, the number of states per energy goes as the square-root of the energy. In this case we have[2]

$$g_c(E) = \frac{4\pi \left(2m_n^*\right)^{3/2}}{h^3} \sqrt{E - E_c} \qquad (2)$$

and

$$g_v(E) = \frac{4\pi \left(2m_p^*\right)^{3/2}}{h^3} \sqrt{E_v - E} \qquad (3)$$

where $g_c(E)$ is the density of states for free electrons, $g_v(E)$ is the density of states for holes, m_n^* the effective mass of an electron, m_p^* the effective mass of a hole, E_c is the energy of the bottom of the conduction band, E_v is the energy at the top of the valence band. Finally the curves at the top are the product of the probability distribution with the density of states which yields the carrier densities as a function of energy. The integral of these curves over energy will give the total number of carriers per unit volume. In semiconductor engineering the unit volume is cm^3, so I follow this tradition.

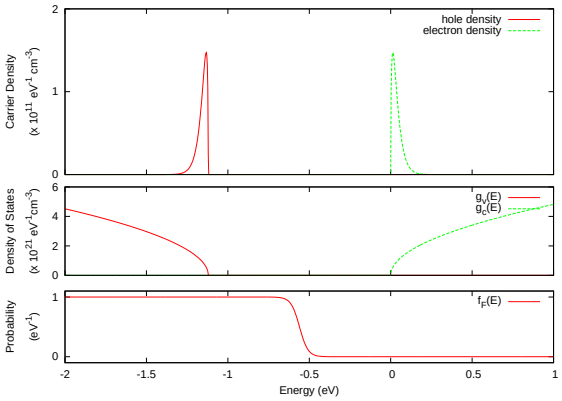

Figure 2: Calculation of carrier densities in silicon at 300 K.

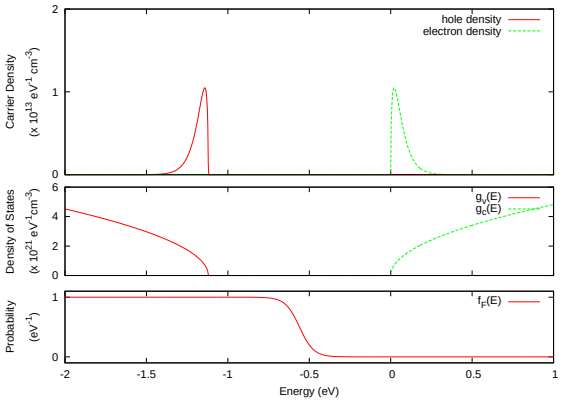

Figure 3: Calculation of carrier densities in silicon at 500 K.

What I had previously asserted about the Fermi energy requires a certain qualification now. Since each free electron in an electrically neutral piece of semiconductor will have a corresponding hole, the area of the two distributions must be equal. If the effective masses of the electron and hole are the same, this results in the Fermi energy E_F being at the center of the band gap. If the effective mass of the hole is greater than that of the electron, then E_F will drop slightly below the mid-point.

The number of free electrons in pure silicon at room temperature is 1.0×10^{10} cm^{-3}, while the number of silicon atoms is 2.9×10^{19} cm^{-3}.[3]

1.1.1 Doping

Very interesting things happen if one mixes very small amounts of dopant into the semiconductor. If phosporus (^{15}P) is mixed into molton silicon at a concentration of 340 ppm, this will result in a density of 10^{16} cm^{-3} of phosphorus atoms in the resulting crystal. Phosphorus has one more valence electron than silicon, however it will be sitting at a location in the crystal which is a perfect fit for silicon, this will result in the extra electron being very poorly bound to the phosphorus atom, it will require very little energy to remove it, promoting it into the conduction band of the silicon bulk. Unlike the promotion of a silicon electron to the conduction band, this does not result in a mobile hole — the hole can not move to a silicon atom because the energies don't match. Due to the ease with which phosphorus gives up its electron, it is called a donor site. The phosphorus doped silicon is called *n-type* semiconductor.

Figure 4 shows the effect of phosphorous doping on the carrier densities. Notice how the Fermi energy has moved up towards the valence band. The integral of the distribution is effectively the same as the dopant concentration, indicating that as expected, each phosphorus atom has indeed given up its electron. The amount by which E_F is shifted is given by[2]

$$\phi_{Fn} = \frac{-kT}{e} \ln \frac{N_d}{n_i}, \tag{4}$$

where $e\phi_{Fn}$ is the energy shift in the Fermi energy due to doping, N_d is the donor concentration, n_i is the intrinsic (undoped) carrier concentration, and e is the charge of an electron.

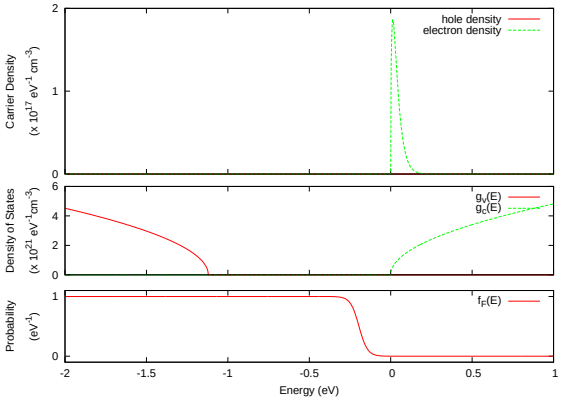

Figure 4: Calculation of carrier densities in silicon at 300 K doped with a 10^{16} cm^{-3} concentration of phosphorus.

In an n-type semiconductor the electrons are called majority carriers and holes are minority carriers.

The opposite phenomena occurs when doping silicon with boron (^{13}B), since boron is sitting with 4 silicon neighbours, each of whom wishes to share an electron, boron will willingly steal a thermally created electron in an effort to fit in. This will leave the corresponding hole free. This makes boron an acceptor, boron doped silicon is *p-type* semiconductor. Carrier densities are shown in figure 5. This time the Fermi energy has moved down towards the valence band. The shift is given by

$$\phi_{Fp} = \frac{kT}{e} \ln \frac{N_a}{n_i}, \tag{5}$$

where $e\phi_{Fp}$ is the energy shift in the Fermi energy due to doping, N_a is the acceptor concentration, and n_i is the intrinsic (undoped) carrier concentration.

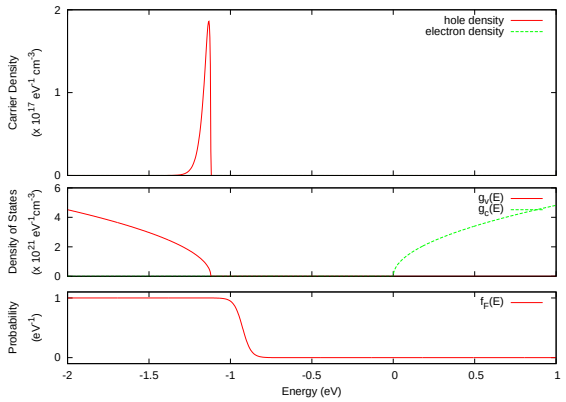

Figure 5: Calculation of carrier densities in silicon at 300 K doped with a 10^{16} cm^{-3} concentration of boron.

In an p-type semiconductor the holes are called majority carriers and electrons are minority carriers.

1.1.2 Current in a semiconductor

If an electric field is applied across a piece of semiconductor, the free charge carriers are accelerated, however a charge carrier will not travel too far before having an inelastic collision. The result is that the entire collection of charge carriers *drift* in the direction of acceleration. For low electric fields the *drift velocity* is proportional to the electric field

$$v_{dp} = \mu_p E \tag{6}$$

and

$$v_{dn} = \mu_n E, \tag{7}$$

where v_{dp} and v_{dn} are the drift velocities of the holes and electrons respectively, and μ_p and mu_n are the *hole mobility* and *electron mobility* respectively.

The total current in a semiconductor is the sum of hole current and electron current.

1.2 P-N Junction

Today almost all p-n junctions are created by different stages of ion implantation or diffusion of dopant into a substrate, however this results in less than trivial junction geometry, therefore harder math. Conceptually it is easier to consider our two flavors of doped silicon brought together in electrical contact.

In order to describe what happened in the junction we must construct the band structure of the junction. Life is

particularly simple in this case, because the band gap of our two materials is the same (doping does not change the band gap significantly). The first rule which is applied is that the Fermi energies of the two material in contact must be the same. Then the conduction and valence bands need to be joined up. Figure 6 shows a sketch of this with appropriately shakily drawn valence and conduction bands. Qualitatively we can see that far away from the junction, the carrier concentrations will be as previously described for the p-type and n-type semiconductor, also at the point where E_F is at the midpoint of the band gap we will have the same carrier concentrations as in the undoped semiconductor.

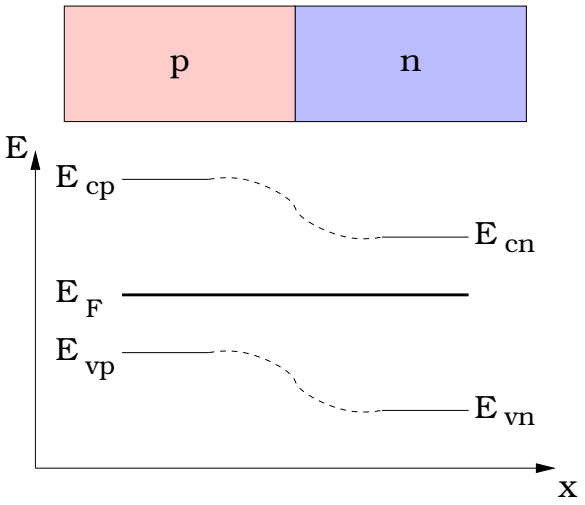

Figure 6: Sketch of band structure of p-n junction.

In a more qualitative treament, having chosen functions to join the valence and conduction bands, we can calculate the carrier distribution as a function of x. This is shown in the top trace in figure 7. The middle trace is the density distribution of the fixed charges due to the $^{13}B^-$ and $^{15}P^+$ ions. Finally, the lower trace is the net charge distribution.

The first observation is that the region around the junction itself has been swept free of carriers, this region is called the *depletion region*. Actually, it is incorrect to say that they have been swept out, a check of the total charge density will show that they have disappeared — this is because when electrons and holes meet they tend to annihilate, producing a photon of energy similar to the band gap. A thorough energy accounting should show that the energy loss via photons would be the work required to separate the two pieces of semiconductor.

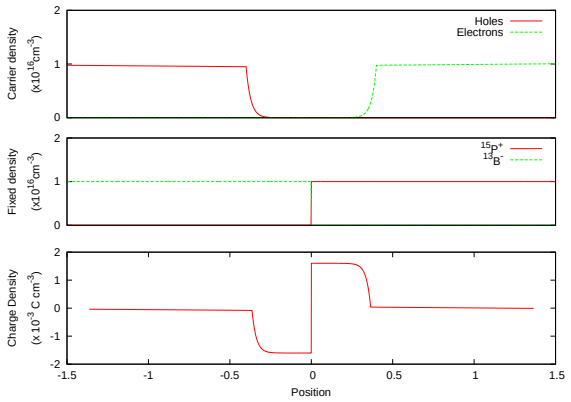

Figure 7: Spatial distribution of charges in p-n junction.

Given that we now have a net charge distribution, we can calculate the electric field and potential using Poisson's equation[2]

$$\frac{d^2\phi(x)}{dx^2} = \frac{-\rho(x)}{\epsilon_s} = -\frac{dE(x)}{dx}, \qquad (8)$$

where $\phi(x)$ is the electric potential, $E(x)$ the electric field, $\rho(x)$ is the volume

charge density, and ϵ_s is the permittivity of the semiconductor. However we already know that the the n side of the junction is more positive than the p side by $\phi_{Fn} - \phi_{Fp}$, so this really gives us the dimension scale.

$$W = \sqrt{2\epsilon_s \left(\phi_{Fn} - \phi_{Fp}\right) \left[\frac{N_a + N_d}{N_a N_d}\right]}, \qquad (9)$$

where W is the width of the depletion region. For the example given the width of the depletion region is about 60 nm.

For those who are troubled by the fact that a p-n junction has a potential across it when no current is flowing, which does not reflect our experience with measuring the voltage across a diode, consider that in order to measure this voltage one needs to attach metal to the ends of the semiconductor. Particularly challenging is the p-type semiconductor, where one needs to convert holes into electrons — in a non rectifying manner. One of the practical chalenges is making *ohmic contacts*, that is contacts in which the voltage drop varies linearly with current. The act of soldering may be diffuse the metals in the solder into the semiconductor, which is in effect doping which may create an unwanted p-n junction at the contact.

1.2.1 Current in a P-N Junction

In order to pass a current through the semiconductor, this current must pass through all regions, that is in the p-type region it will be carried by holes, in the n-type region it is carried by electrons, in the region of the junction — magic.

If we pass a current in the *forward* direction, we have electrons drifting towards the junction in the n-type, and holes drifting towards the junction in the p-type. This results in mutual annihilation in the region of the junction.

Attempting to pass current in the reverse direction is much harder, the best we can do is pull thermally created carriers out of the depletion region.

The relation of voltage drop to current is given by,[2]

$$I = I_s \left[e^{\left(\frac{eV_a}{kT}\right)} - 1\right], \qquad (10)$$

where I_s is the reverse diode saturation current density, e the charge on the electron, k the Boltzman Constant, T the temperature (Kelvin), and V_a is the voltage across the junction. $\frac{kT}{e}$ = 25.9 mV at 300 K.

In practice, there is a small factor which is added to model the behavior of real diodes:

$$I = I_s \left[e^{\left(\frac{eV_a}{nkT}\right)} - 1\right], \qquad (11)$$

where n is called the *niceness factor*, which has a range of 1 to 2, 1 being the nicest, and 2 being more frequently observed.

1.3 Light Emitting Diode

Recall that when current is flowing, holes and electrons are mutually annihilating one another in the region of the junction. The energy liberated, which will be at minimum the band gap energy, will be liberated as either a photon or a phonon (lattice vibration). If one constructs the p-n junction appropriately, then photons created at the junction can escape the material. PN junctions created for this purpose are called *light emitting diodes* or LED. The color of an LED is determined by the band gap, in the case of silicon, with a band gap of 1.12 eV we get a photon of 1107 nm which is in the infrared. In order to get band gap which coincide with the visible spectrum, we need to make semiconductors which are non elemental crystals, for example gallium arsenide phosphide ($GaAs_{1-x}P_x$), aluminium gallium indium phosphide (AlGaInP) and gallium phosphide (GaP).

Recall that in the region where photons are being produced, that E_F is close to the mid-point between the valence and conduction bands, thus the carrier energy distributions are not dissimilar to those of intrinsic semiconductor, as shown in figure(2). Given that the electron comes from somewhere in the conduction band and the hole from somewhere in the valence band, the distribution of energies liberated by their mutual annihilation can be calculated. By eye, this would look to be of order 0.1 eV, which yields a spread of 5% in the wavelength. This is consistent with observation.

1.4 LASER Diode

Since modern semiconductor manufacture uses a single crystal which is cleaved along crystalographic planes, it is possible to use these planes as mirrors which are parallel at an atomic scale. Figure 8 shows a schematic of a broad-area junction laser. The cleaved facets at the left and right act as mirrors which create an optical cavity. The reflectivity of the mirror plane is a function of the refractive index of the semiconductor and of air.[3]

$$R = \left(\frac{n_{\mathrm{s}} - n_{\mathrm{a}}}{n_{\mathrm{s}} + n_{\mathrm{a}}}\right)^2 \tag{12}$$

For GaAs $N_{\mathrm{S}} = 3.6$, this would give a reflectivity of 0.32. It is noted that this is tiny when compared to the partial mirrors on a HeNe laser where $R > 0.9$.

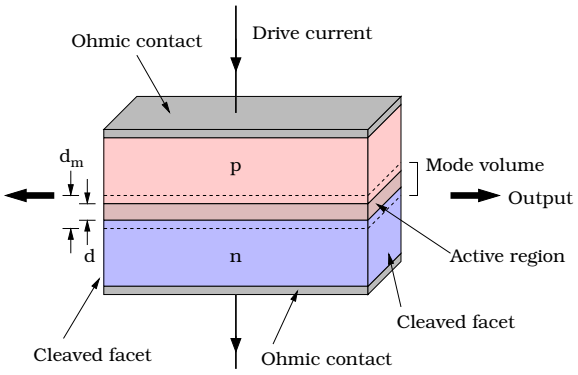

Figure 8: Construction of a broad-area junction laser with cleaved facets[3].

In active region where holes and electrons are annihilating one another, photons are being generated in all

directions initially, some will cause stimulated emission, generating a second photon with the same characteristics (polarization, wavelength and direction) as the initial photon, however, photons which are reflected back into the region by the mirroring effect of the cleaved facets have a much higher probability of causing stimulated emission. Since an electron-hole hole pair which has been destroyed by stimulated emission has been eliminated, it can not generate a photon with random characteristics, thus a prefered direction of emission is established — this is the onset of lasing. The current at which lasing begins is called the *threshold current*.

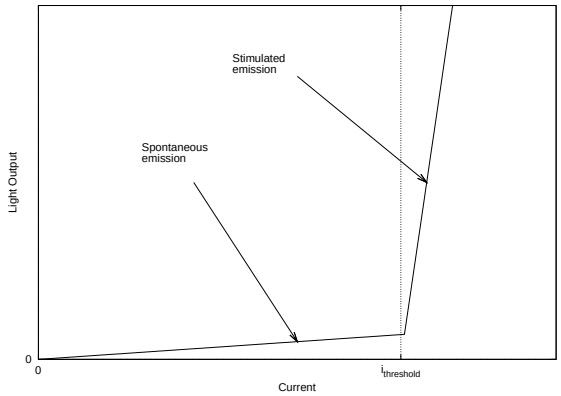

Figure 9: Light output-current characteristic of an idea semiconductor.[3].

Below the threshold current, light output is dominated by spontaneous emission, which like the LED, has a spread of about 5% upon the wavelength. However, when lasing the distribution of wavelength in the light output will be much sharper. Since the reflectivity of the mirrors is not terribly high, it is not obvious that the length of the cavity plays a strong role in wavelength selection.

2 Polarizer

A simple polarizer is a grid of parallel wires as shown in figure(10). Light at the right of the grid has randomly oriented electric field. Photons having an electric field in the y direction will accelerate electrons along the length of the wire, converting photon energy into joule heating. Thus photons having an electric field parallel to the wires are absorbed, while photons with electric fields perpendicular to the wires will pass unattenuated.

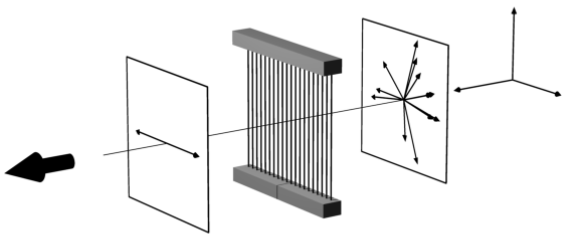

Figure 10: Wire-grid polarizer[4]

The polarizers we use are manufactured by heating a sheet of polyvinyl alcohol and stretching it in a given direction.[4] This causes the long hydrocarbon molecules to become aligned along the direction of stretching. Since hydrocarbons are not good conductors,

this does not a polarizer make. When the plastic is soaked in an ink rich in iodine, the iodine attaches to the hydrocarbon chains and it is the iodine conduction electrons which absorb the photons.

3 Malus's Law

Malus's Law describes the intensity of light passing through two polarizers as a function of the angle between the directions of conduction of the two polarizers.

$$I(\theta) = I(0)\cos^2\theta \tag{13}$$

See Appendix B on how you can determine the best estimates of the parameters from your data.

4 Refraction

When light passes from one medium to another, the wave vector is refracted by an angle dependent upon the refractive indexes of the two medium. A rather lopsided rendering of such an transition is shown in figure(11).

The relationship between the angles of incident and transmitted light, θ_i and θ_t and the refractive indexes of the media, n_i and n_t are described by Snell's Law

$$n_i \sin\theta_i = n_t \sin\theta_t \tag{14}$$

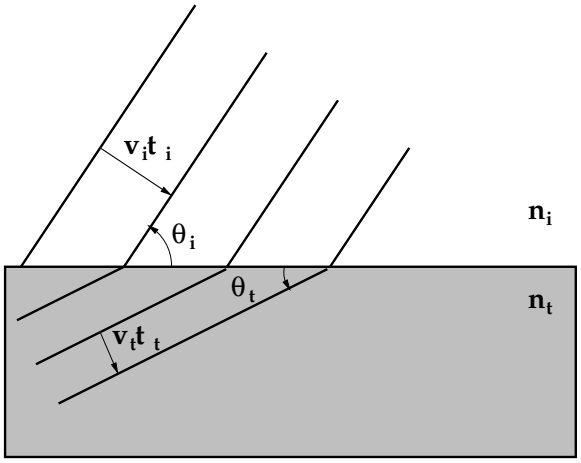

Figure 11: Refraction of light an an interface between two mediums.

5 Reflection

Some light is reflected when light passes from one medium to another, the relationships are different for light which is polarized parallel to the plane of incidence and for light which is polarized perpendicular to the plane of incidence. In summary[4]

$$R_{\parallel} = \frac{\tan^2(\theta_i - \theta_t)}{\tan^2(\theta_i + \theta_t)} \tag{15}$$

and

$$R_{\perp} = \frac{\sin^2(\theta_i - \theta_t)}{\sin^2(\theta_i + \theta_t)} \tag{16}$$

These relationships are shown graphically in figure(12) for light passing from a vacuum ($n_i = 1$) into glass ($n_t = 1.5$). Notice how $R_{\parallel}$ dips down to zero at about 57°, this is Brewster's angle. This will correspond to a maximum of the transmitted light, since neglecting attenuative losses in the slide

$$T = 1 - R \tag{17}$$

It should be evident from figure(12) that you will need to be careful to align the polarization of the incident light with the plane of incidence. Hint, you can use the disappearance of $R_{\parallel}$ at Brewster's angle to know when you are right.

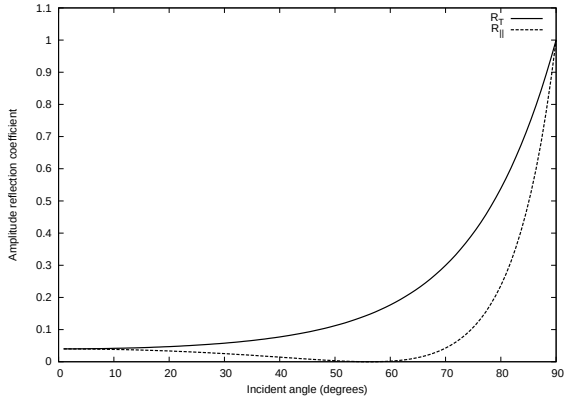

Figure 12: Coefficients of reflection for light parallel ($R_{\parallel}$) and perpendicular ($R_{\perp}$) to the plane of incidence.

Examining eq(15), one can see that the zero results from $\tan^2(\theta_i + \theta_t)$ diverging to infinity, which will occur when $\theta_i + \theta_t = \frac{\pi}{2} + i\pi$, where i is an integer. Since θ_i and θ_t may not be physically larger than $pi/2$, we have only to solve

$$\theta_i + \sin^{-1}\left(\frac{n_i}{n_t}\sin\theta_i\right) - \frac{\pi}{2} = 0 \qquad (18)$$

Algebraically a pain, it can easily be done numerically.[2] The results are shown in figure(13). The range 1 to 4 spans most observed materials from vacuum to silicon.

[2]See Appendix C

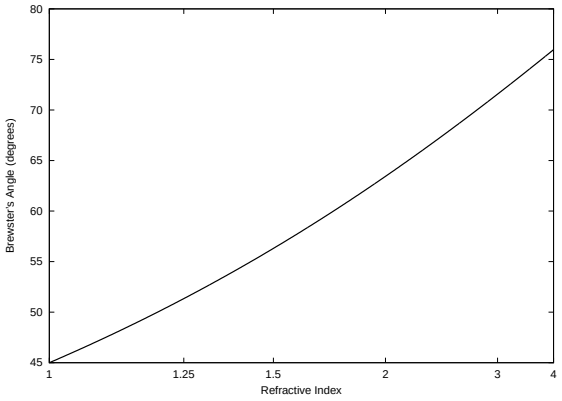

Figure 13: Brewsters angle, numerically computed for range of refractive indices $1 \leq n_t \leq 4$. Note, the x-axis has been linearized to $-1/n_t$.

6 The Sensor Circuit

The light intensity sensor is an **OP804**[3] phototransistor. A phototransistor works like a normal transistor, with the base current provided by the photocurrent produced in the base-collector junction.

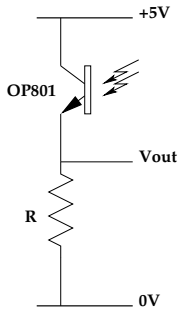

Figure 14: Schematic of sensor circuit

[3]The technical specifications are attached as an appendix

Figure 14 shows how the phototransistor is connected. When in an unsaturated state the collector current is proportional to the intensity of light falling upon the active region of the transistor.

$$i_c = \mathrm{gI} \tag{19}$$

The resistor converts this current to a voltage drop,

$$V_{out} = i_c R \tag{20}$$

If the resistance is too small the output signal will be very small, remember the ADC in the Labmaster is precise to 5mV. If the resistance is too large, then the current necessary to satisfy equation 19 would result in a voltage drop greater than the supply voltage in equation 20, obviously this will not happen.

7 The Stepper Motor

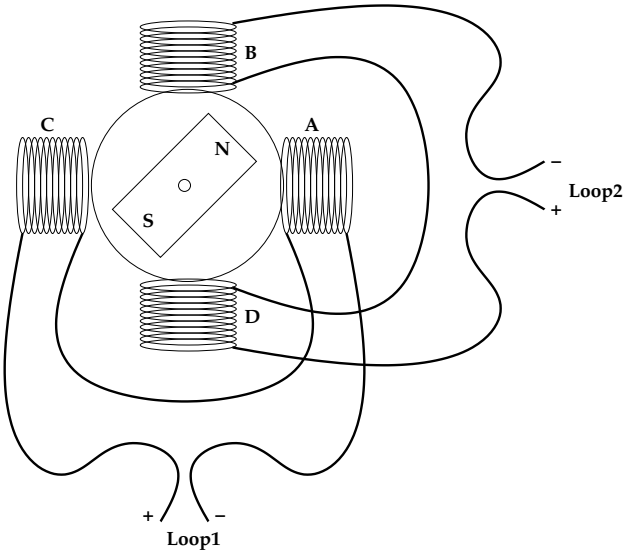

Figure 15: Block diagram of a stepper motor

Figure 15 shows a block diagram of a stepper motor. At the center is a permanent magnet which is free to rotate about the central axis. Let coils **A** through **D** be wired such that if current is applied to **Loop1** observing the indicated polarities, the inner pole of coil **A** is south, and the inner pole of coil **C** is north; similarly for loop **Loop2**, the inner pole of coil **B** is south, and the inner pole of coil **D** is north. Thus the permanent magnet is at equilibrium as shown. If the polarity of the current through **Loop1** is now reversed, the permanent magnet will rotate 90° clockwise to a new equilibrium position. Now reversing the current through **Loop2**, the magnet again rotates 90° clockwise. Returning the current in

Loop1 to its original polarity, the magnet rotates another 90° clockwise. Finally returning the current in **Loop2** to its original polarity, the magnet proceeds again, returning to its starting position. It is clear that if these steps are reversed that the magnet will rotate counter-clockwise. Thus by alternating the polarities of the currents in the two loops in a set pattern that the magnet may be rotated in a desired direction.

Since there is power applied to the stepper motor while it is motionless it will tend to get hot. Try not to leave the motors powered when they are not in use.

8 Stepper Motor Controller

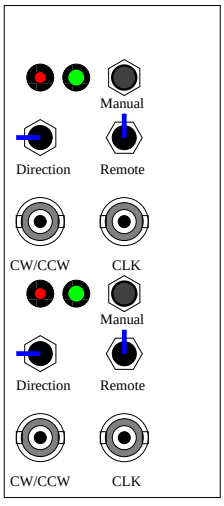

Figure 16: Front panel of stepper motor controller

Figure 16 shows the front panel of the stepper motor controller. Each controller has two independant control units. Each unit can be used in manual, or in remote mode.

Manual mode is selected by placing the **Manual/Remote** switch in the lower position. The **Direction** switch controls the direction, pressing the push-button will actually move the motor.

Remote mode is selected by placing the **Manual/Remote** switch in the upper position. The direction of rotation is selected by the TTL level applied to the BNC input **CC/CCW** (clockwise / counter-clockwise). Upon each rising edge applied to the BNC input **CLK** the motor will advance one step.

9 Software

On the Wiki you will find find a small program `laser.c` which will demonstrate the use of the stepper motor.

10 Knife Edge

In order to gain precision in the measurement of the beam profile, notice that you can angle the knife blade with respect to the direction of travel. You might consider the geometry shown in figure 17 where the knife-edge $\vec{AB}$ is traveling horizontally through the beam at velocity $\vec{v}$, however, if the knife-edge is

considered only as a line, this line advances with velocity $\vec{k}$. Simple geometry reveals the relationship between $\vec{k}$, $\vec{v}$, and the angle between these vectors.

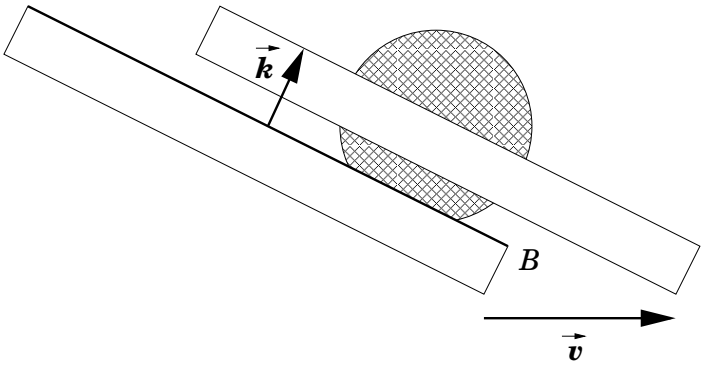

Figure 17: Knife edge moving through laser beam

A Derivation of Doppler Spread of Spectral Lines

Given the Boltzmann distribution,

$$\frac{N_i}{N} = \frac{g_i e^{-E_i/k_b T}}{\sum_j g_j e^{-E_j/k_b T}} \tag{21}$$

and that

$$E = \frac{p^2}{2m} \tag{22}$$

and borrowing from the quantum mechanical result for a particle in a box that momentum will be quantified, such that $p_x = n_x \Delta p^x$, $p_y = n_y \Delta p_y$ and $p_z = n_z \Delta p_k$, where n_x,n_y and n_z are quantum numbers, since the particles are independent, each may have the same quantum number simultaneous, so $g_i = N$ for all i;

$$\frac{N_i}{N} = \frac{N e^{-i^2 \Delta p_x^2/2mk_bT}}{\sum_j N e^{-j^2 \Delta p_x^2/2mk_bT}} \tag{23}$$

Switching to integral form,

$$\int_{p_x 1}^{p_x 2} P(p_x) dp_x = \int_{p_x 1}^{p_x 2} \frac{e^{-p_x^2/2mk_bT}}{\int_{-\infty}^{\infty} e^{-p_x^2/2mk_bT} dp_x} dp_x \tag{24}$$

$$\int_{p_x 1}^{p_x 2} P(p_x) dp_x = \int_{p_x 1}^{p_x 2} \frac{e^{-p_x^2/2mk_bT}}{\sqrt{2\pi mk_bT}} dp_x \tag{25}$$

This can be trivially rewritten for v_x since $p_x = mv_x$,

$$\int_{v_x 1}^{v_x 2} P(v_x) dv_x = \sqrt{\frac{m}{2\pi k_b T}} \int_{v_x 1}^{v_x 2} e^{-mv_x^2/2k_bT} dv_x \tag{26}$$

Figure(18) show an atom travelling with velocity v along the x-axis which emits a photon as it passes the point $x = 0$, after one period, τ, the atom has reached $x = v\tau$ while the wave front of the photon has reached $x = c\tau$. Thus, the period of the doppler shifted photon will be,

$$\lambda = c\tau - v\tau, \tag{27}$$

where

$$\tau = \gamma \frac{hc}{E} \tag{28}$$

where γ is the Lorentz factor. It really is not necessary to treat this relativistically, but it does no harm either.

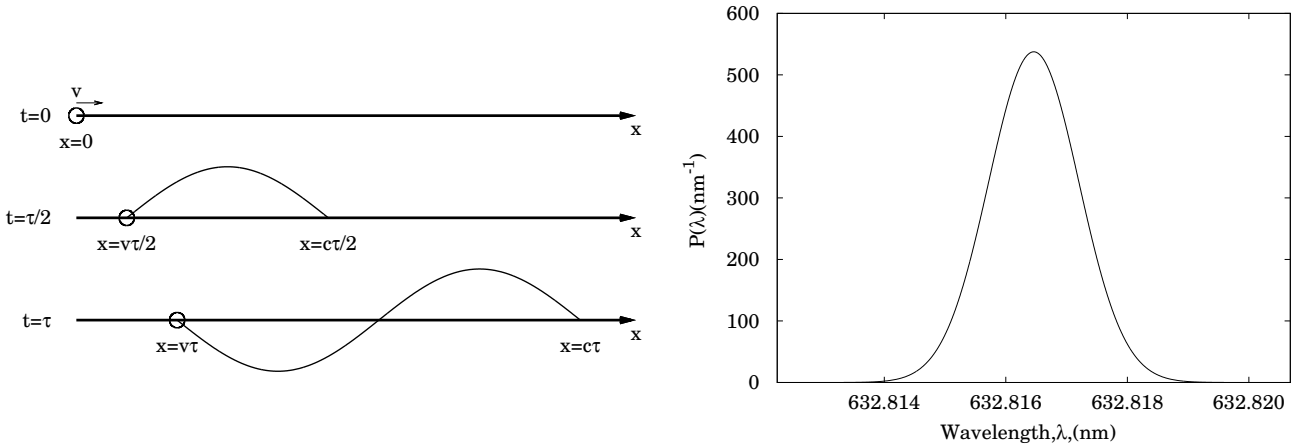

Figure 18: Doppler shift due to atom emitting photon while moving at velocity v along x-axis and the resulting distribution of wavelengths for neon $5s \rightarrow 3p$

For a photon emitted parallel to the x-axis, from an atom moving with velocity v_x at the instant it passes the origin, the electric field at the location of the atom will be

$$E(vt) = E_0 sin\omega t \tag{29}$$

Since this E-field propagates along the x-axis at speed c,

$$E(vt + x) = E_0 sin\left(\omega(t - \frac{x}{c})\right) \tag{30}$$

then

$$E(x) = E_0 sin\left(\omega(t - \frac{x - vt}{c})\right) \tag{31}$$

Which rewritten in a more canonical form is

$$E(x) = E_0 sin\left(\omega(t - \frac{x - vt}{c})\right) \tag{32}$$

B Fitting to Malus's Law

Given Malus's Law,

$$I(\theta) = I(0)\cos^2\theta \tag{33}$$

You have a set of measurements V_i. Which were taken under the following conditions, laser beam passed through 1 or more polarizers, the direction of polarization of the last of these polarizers, ϕ_{f}, is arbitrarily set; the beam next passes

through your rotating polarizer which before stepping was set to polarization direction ϕ_m; the intensity of the resulting beam is then converted to a voltage by the phototransistor. The relation here will be

$$V_i = \alpha I_i, \tag{34}$$

where α is a property of the phototransistor circuit. Given that you know the angular size, ω_m, of each step of the stepping motor assembly, the angle between the polarizers in eq(33) is given by

$$\theta_i = \phi_m - \phi_f + \omega_m i \tag{35}$$

For your purposes, ϕ_m and ϕ_f are not interesting, so we can replace them with a single phase-shift, ϕ. Thus, the χ^2 of our fit to the data will be

$$\chi^2 = \sum_{i=1}^{N} \left(\frac{V_i - \alpha I(0) \cos^2(\omega_m i + \phi)}{\sigma_i} \right)^2 \tag{36}$$

Since we don't know $I(0)$ we can not solve for α. Since we don't care about the value of α, we can make the following substitution, $V_0 = \alpha I(0)$. The partials we need to set to zero for minimization then become,

$$\frac{\partial \chi^2}{\partial V_0} = 2 \sum_{i=1}^{N} \left[\frac{-V_i \cos^2(\omega_m i + \phi) + V_0 \cos^4(\omega_m i + \phi)}{\sigma_i^2} \right] = 0 \tag{37}$$

$$\frac{\partial \chi^2}{\partial \phi} = 4 V_0 \sum_{i=1}^{N} \frac{(V_i - V_0 \cos(\omega_m i + \phi)^2) \cos(\omega_m i + \phi) \sin(\omega_m i + \phi)}{\sigma_i^2} = 0 \tag{38}$$

Neither of these equations solve themselves, so we must use an iterative method to reduce the χ^2. Notice that if ϕ is known, then eq(37) can be solved for V_0. Since the first few data points are dubious, due to the ugly startup of the stepping motor, we might as well cut the data to start at the first maxima of the voltage readings, this means our first guess at ϕ is zero. From this we can calculate V_0

$$V_0 = \sum_{i=1}^{N} \frac{V_i \cos^2(\omega_m i + \phi)}{\sigma_i^2} / \sum_{i=1}^{N} \frac{\cos^4(\omega_m i + \phi)}{\sigma_i^2} \tag{39}$$

For the next step, we need to determine a new guess of ϕ which will minimize eq(36). One trick we can use is to assume that χ^2 is parabolic near its minima. Thus, we perform a quadratic Taylor Expansion of $\chi^2(\phi)$ around our current guess for ϕ. We already have an expression for $\partial \chi^2 / \partial \phi$ in eq(38).

$$\frac{\partial^2 \chi^2}{\partial \phi^2} = 12 V_0^2 \sum_{i=1}^{N} \frac{\cos^2}{\sigma^2} - 16 V_0^2 \sum_{i=1}^{N} \frac{\cos^4}{\sigma^2} - 4V0 \sum_{i=1}^{N} \frac{V_i}{\sigma^2} + 8 V_0^2 \sum_{i=1}^{N} \frac{V_i \cos^2}{\sigma^2} \tag{40}$$

For a Taylor expansion

$$f(x) = \sum_{n=0}^{\infty} \frac{f^{(n)}(a)}{n!}(x-a)^n \tag{41}$$

For a quadratic

$$y = ax^2 + bx + c, \tag{42}$$

the minima will occur at

$$x = -\frac{b}{2a} \tag{43}$$

which in our case will be

$$\phi_{i+1} = \phi_i - \frac{\partial \chi^2}{\partial \phi}(\phi_i) / \frac{\partial^2 \chi^2}{\partial \phi^2}(\phi_i) \tag{44}$$

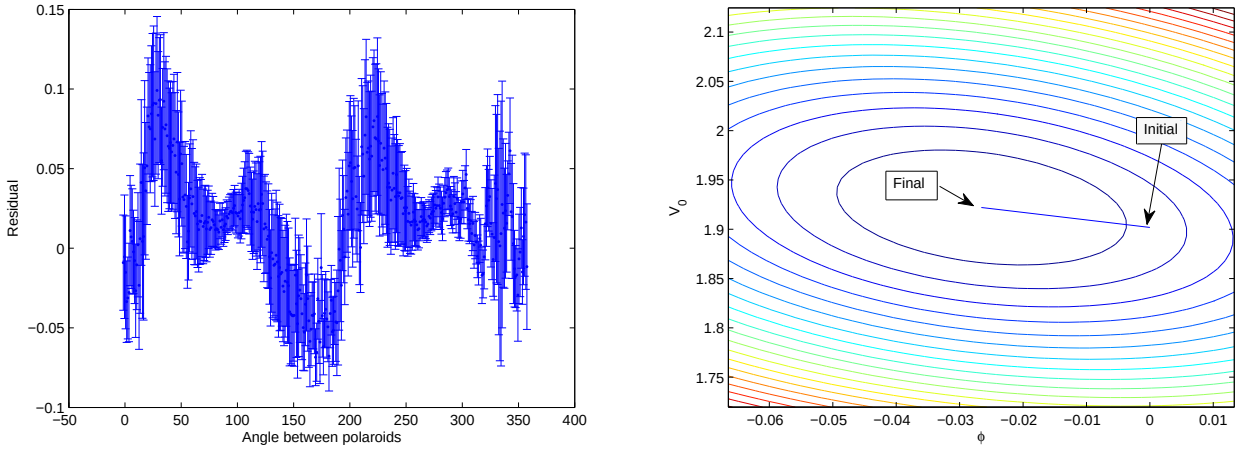

Figure 19: Residual after fitting and contour plot of $\chi^2(\phi, V_0)$ in the region of best fit with path taken to best fit.

As can be seen, the residual of the best fit clearly has a trend. This can not be blamed upon the fit parameters not being optimal since there is clearly a higher spatial frequency component present.

B.1 Script to minimize χ^2 for Malus's Law

```
clear
load 'malus.mat' % raw data
```

```
load 'adc.mat'       % calibration constants

w = pi/180;

v_long = m_adc0 * malus_adc0 + b_adc0;


% Cut initial dynamics from data
% ... and start roughly at a maxima
skip=55;
v = v_long(skip:end);

% fold up the data
for row = 1:floor(length(v)/360)
  data(row,:) = v(1+(row-1)*360:row*360);
end
i = [0:359];
s = sqrt(var(data)+0.01^2);

errorbar(w*i,max(data),s,'.')
v = max(data);

phi = 0; % initial guess
for j = 1:10 % arbitrary number of iterations

  coswiphi = cos(w*i+phi); % somehow it feels more efficient
  sinwiphi = sin(w*i+phi); % to precalculate these

  V0 = sum (v.*coswiphi.^2./s.^2) / sum (coswiphi.^4./s.^2);

  chi2 = sum((v - V0.*coswiphi.^2).^2./s.^2);

  dchi2dphi = 4*V0*sum((v-V0.*coswiphi.^2) ...
                           .*coswiphi.*sinwiphi./s.^2);

  d2chi2dphi2 = 12*V0^2*sum(coswiphi.^2./s.^2) ...
              - 16*V0^2*sum(coswiphi.^4./s.^2) ...
              - 4*V0*sum(v./s.^2) ...
              + 8*V0*sum(v.*coswiphi.^2./s.^2);

  phis(j) = phi; % save values for later
  V0s(j) = V0;   % postmortem
```

```
  chi2s(j) = chi2;
  dchi2s(j) = dchi2dphi;
  d2chi2s(j) = d2chi2dphi2;
  [ chi2, phi V0 ] % show intermediate values
  % update guess
  phi = phi - (dchi2dphi) / (2*d2chi2dphi2/2);
end

figure(1)
errorbar(180*(w*i+phi)/pi, v - V0 * cos(w*i+phi).^2,s,'.')
xlabel('Angle between polaroids');
ylabel('Residual');

% This bit just generates the contour plot
% in the region of best fit
dphi = max(abs(phis-phis(end)))*1.5;
dV0 = max(abs(V0s-V0s(end)))*10;
phi_v = linspace(phis(end)-dphi,phis(end)+dphi,50);
v0_v = linspace(V0s(end)-dV0,V0s(end)+dV0,50);
for j=1:length(phi_v)
  coswiphi = cos(w*i+phi_v(j));
  for k=1:length(v0_v)
    chi2_m(k,j) = sum((v - v0_v(k).*coswiphi.^2).^2./s.^2);
  end
end

figure(2)
contour(phi_v, v0_v, chi2_m,20)
hold on
plot(phis,V0s)
xlabel('\phi')
ylabel('V_0')
```

C Newtons Method to solve Brewster's Angle

```
function theta_i = newton_brewsters (n_t)
  n_i = 1;
  for i = 1:length(n_t)
    theta_i(i) = pi/4; % starting guess
```

```
    for j = 1:10
      error = theta_i(i) ...
              + asin(n_i/n_t(i)*sin(theta_i(i))) ...
              - pi/2;
      if error == 0
        break
      end

      numer = n_i * cos(theta_i(i));
      numer2 = n_i^2*sin(theta_i(i))^2;
      denom2 = n_t(i)^2;
      denom = n_t(i) * sqrt(1 - numer2/denom2);
      derror_by_dtheta_i = 1 + numer / denom;

      theta_i(i) = theta_i(i) ...
                   - error ./ derror_by_dtheta_i;
    end
  end
end
```

References

[1] N. David Mermin Neil W. Ashcroft. *Solid State Physics*. W. B. Saunders, 1976.

[2] David A. Neamen. *Semiconductor Physics and Devices — 3rd ed.* McGraw-Hill, 2003.

[3] Pallab Bhattacharya. *Semiconductor Optoelectronic Devices — 2nd ed.* Prentice Hall, 1993.

[4] Eugene Hecht. *Optics*. Addison-Wesley Publishing Company, 1989.